Virchows Arch A (1987) 410:433–441

Virchows Archiv A


# Stereology and flow-cytometry of well-differentiated follicular neoplasms of the thyroid gland

**Torsten Mattfeldt**[1], **Guido Schürmann**[2], **and Georg Feichter**[1]

[1] Pathologisches Institut der Universität Heidelberg, Im Neuenheimer Feld 220/221, D-6900 Heidelberg, Federal Republic of Germany

[2] Chirurgische Abteilung der Universität Heidelberg, Im Neuenheimer Feld 111, D-6900 Heidelberg, Federal Republic of Germany

**Summary.** A retrospective analysis of surgically resected thyroid nodules by stereology and DNA flow cytometry was performed in 15 follicular adenomas and 15 well-differentiated follicular carcinomas. The criteria for diagnosis were based on the WHO classification of thyroid tumours. By area-weighted random sampling of the visual fields for light-microscopic stereology, any subjective selection bias was precluded, and each point within the embedded neoplastic tissue was given equal probability of being analyzed. 150–250 tumour cell nucleus (TCN) profiles were studied per case by a semiautomatic image analyzing system. Flow cytometric analyses included measurement of the DNA-index, and the percentages of cells in S-phase and in G2/M-phase. Adenomas and carcinomas did not differ in stereological estimates related to TCN size. As examination of the stereological techniques by nested analysis of variance showed that this result cannot be ascribed to inaccurate methods, it follows that determination of TCN size is not a useful tool for the diagnosis of malignancy in well-differentiated thyroid tumours. Both groups included similar proportions of diploid and aneuploid neoplasms. In the carcinoma group the percentage of tumour cells in the G2/M-phase was more than twice as high than in the adenoma group ($P<0.01$). The ratio of short to long TCN profile axis was significantly smaller, and the coefficient of variation of TCN profile area was significantly higher in carcinomas than in adenomas. These findings are consistent with more unequiaxed TCN and higher anisokaryosis in the malignant tumours. Despite the significant differences, however, overlap of data from individual cases precludes the use of these estimates as diagnostic criteria. Pooling of the follicular tumours and dichotomizing the sample by the DNA-index showed that mean TCN profile area is increased and surface-to-volume ratio of TCN is decreased in aneuploid as compared to diploid tumours. This finding indicates that aneuploidy is associated with an increase of TCN size.

**Key words:** Flow cytometry – Follicular neoplasms – Microscopy – Morphometry – Stereology – Thyroid gland

*Offprint requests to:* T. Mattfeldt at the above address

## Introduction

In the established histological typing system of thyroid tumours produced by the WHO (Hedinger and Sobin 1974), follicular neoplasms are classified as follicular adenomas, well-differentiated follicular carcinomas, and moderately differentiated follicular carcinomas. The diagnosis of the moderately differentiated variety can usually be made by experienced pathologists without difficulty. However, the distinction of follicular adenomas with microfollicular, solid or trabecular patterns from well-differentiated follicular carcinomas is intricate because cytological criteria like nuclear atypia or nuclear pleomorphism fail here. Therefore the proper differential diagnosis of well-differentiated follicular neoplasms often necessitates the examination of a large number of sections from resected "cold nodules", because – in the absence of metastases and diffuse infiltrative growth – only capsular infiltration and/or vascular invasion are safe indicators of malignancy (Böcker 1984; Lang et al. 1986). Moreover, this differential diagnosis is impossible from cytological aspirates, hence cytopathologists must in these cases restrict themselves to a global diagnosis of "follicular neoplasia"

(Löwhagen and Sprenger 1974; Droese 1979). In this situation various attempts at a morphometric analysis of follicular neoplasms were made. One group of authors found that morphometry of tumour cell nuclei (TCN) in cytological aspirates permits a preoperative distinction between follicular carcinomas and follicular adenomas with a high statistical probability (Boon et al. 1980; 1982), whereas the majority of investigators could not distinguish between well-differentiated follicular neoplasms from karyometric criteria (Georgii 1977; Lang et al. 1977; Mikuz et al. 1977; Schuh et al. 1980; Droese et al. 1981; Luck et al. 1982; Johannessen et al. 1983; Kriete et al. 1983; Schuh et al. 1984; Kriete et al. 1985). In the present study a combined stereological and flow-cytometric analysis of TCN is performed in resected specimens of follicular adenomas and well-differentiated follicular carcinomas, because sampling errors resulting from aspiration of non-neoplastic thyroid tissue can thus be avoided. Furthermore, this approach provides an opportunity to compare quantitative morphological properties of a tumour with its ploidy and the kinetics of its cell proliferation.

## Materials and methods

The written reports of surgically resected thyroid specimens were screened retrospectively until a total sample of 15 follicular adenomas and 15 well-differentiated follicular carcinomas was completed. The criteria for inclusion into the study were based on the WHO classification of thyroid tumours (Hedinger and Sobin, 1974). Follicular adenomas were only included into the study when they displayed a solid pattern with nuclear irregularities ("atypical" adenomas), or when trabecular, microfollicular or normofollicular growth patterns were found (embryonal, fetal, and simple adenomas), and when there was no clinical evidence for endocrine activity. Thus, pure macrofollicular (colloid) adenomas and autonomous adenomas, which usually offer no diagnostic problems with respect to differentiation from follicular carcinomas, were not included into the study. Moreover, the oxyphilic variants of the well-differentiated follicular neoplasms and the follicular variant of papillary thyroid carcinoma were also excluded from the study (Chen and Rosai, 1977). From all blocks new paraffin sections were cut and stained with hematoxylin/eosin, and these were used for the stereological investigations. After completion of the flow-cytometric studies (vide infra) we reviewed the 6 cases of aneuploid adenomas as a separate group, as suggested by Greenebaum et al. (1985). From each of the 3 small adenomas (maximum diameter $<2.5$ cm) 3–5 paraffin blocks were available, whereas 6–10 blocks had been prepared from the larger adenomas (maximum diameter 3–8 cm). From every block 8 deep step sections were cut and stained with hematoxylin/eosin, elastica/van Gieson, and the Masson-Goldner trichrome stain. The clinical history of these patients was also documented; the follow-up period after resection of the thyroid nodule ranged from 18 months to 5.5 years (mean follow-up period: 3 years).

In resected surgical specimens the sampling process for microscopy includes 2 steps in general: – the sampling of tissue from the whole specimen for embedding, and the subsampling of visual fields on the sections. In our routine work the thyroid specimens are cut systematically into slices and examined macroscopically, and sector-shaped slabs are prepared from thyroid nodules with special attendance to the peripheral tumour regions in order to exclude capsular invasion. It should be emphasized that this sampling step is necessarily not random but part of a diagnostic procedure. From this reason, the number of available sections varied from case to case: whereas an invasive carcinoma could sometimes be detected by a single section, it was often necessary to prepare 8–10 sections for a proper diagnosis of a larger follicular adenoma (Georgii 1977; Lang et al. 1977, 1980, 1986; Böcker 1984). An attempt was made to obtain a strict random sample from the neoplastic follicular tissue on the histological sections. As the available sections

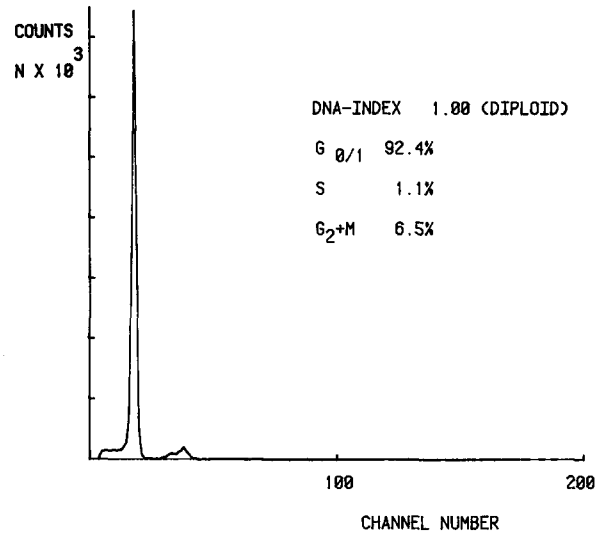


**Fig. 1.** Flow cytometric histogram of a diploid well-differentiated follicular carcinoma (case 8 on the right side of Table 2)

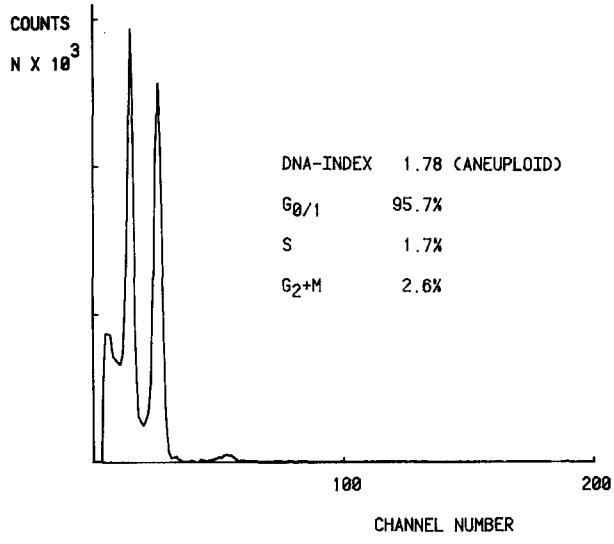


**Fig. 2.** Flow cytometric histogram of an aneuploid follicular adenoma (case 10 on the left side of Table 2). The first peak represents diploid nuclei. A high second peak is clearly discernible which represents an aneuploid cell population

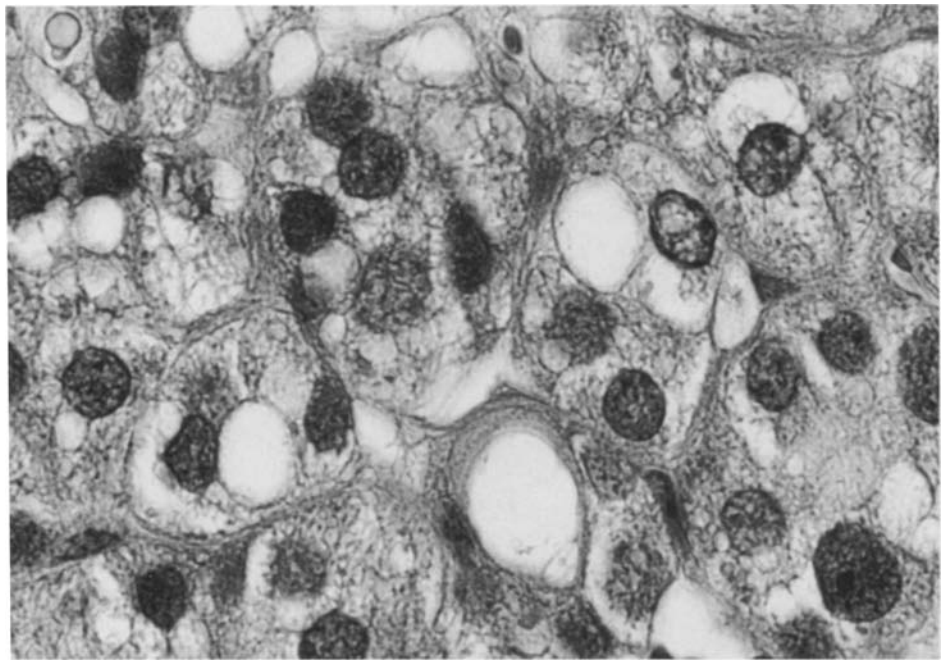

**Fig. 3.** Stereologically analyzed visual field within a follicular adenoma of the thyroid gland. The tumour cell nucleus profiles are well demarcated and can easily be traced by semiautomatic image analyzing systems. Hematoxylin/Eosin. Oil immersion. Final magnification: 1,430×

differ in size, but each point within the embedded neoplastic tissue must have equal probability of being sampled for stereology, area-weighted random sampling was performed which precludes not only any subjective selection bias but also gives the larger sections a higher chance of being studied (Weibel 1979, 1980; Miles and Davy 1976). In practice all technically adaequate slides of a given case were arbitrarily placed on a sheet of transparent paper on which a quadratic lattice with 100 points numbered from 00 to 99 had been drawn (Weibel 1979, p. 79, Fig. 3.11.). Two-digit standard random numbers were drawn from a table (Abramowitz & Stegun, 1964) until 6 points had hit follicular neoplastic tissue. The position of these points was marked with waterproof ink, and the visual fields immediately right to these marks were selected for stereology. The fields were analyzed with a Zeiss light microscope at 1,000× final magnification with oil immersion. By means of a drawing tube connected to the microscope, the TCN profiles were traced with a cursor on a graphic tablet. The raw morphometric data, which included area A, perimeter, long axis, and short axis for each TCN profile, and numerical density of TCN profiles $N_A$ per tumour cell area, were stored on floppy disks in the semiautomatic image analyzing system Kontron MOP-Videoplan. As the tumour cell volume (i.e., the cellular epithelial compartment only) was used as the reference system, the number of points that hit other tumour components (connective tissue, blood vessels, inflammatory infiltrates, empty lumina, colloid) was counted by means of an ocular grid with 100 points in each visual field to correct the raw $N_A$ estimate. It was assumed as the stereological model that the TCN in well-differentiated follicular neoplasm are isotropically oriented particles, as no preferential orientation of the nuclei could be detected. The volume density of TCN per tumour cell volume, $V_V$, was estimated by the Delesse principle: $V_V = N_A *$ (mean TCN profile area). The surface density of TCN per tumour cell volume, $S_V$, was estimated by the equation $S_V = (4/\pi)\ B_A$, where $B_A$ represents the boundary length of TCN profiles per reference area. The surface-to-volume ratio of the nuclei was estimated (separately for each tumour) as the ratio $S_V/V_V$. This parameter – the surface area per unit particle volume – is a general, non-parametric descriptor of size and shape of arbitrary particulate objects; it is inversely related to the mean random secant length through convex particles (Mattfeldt et al. 1985b). If shape remains unchanged, an increase of the surface-to-volume ratio indicates that the objects become smaller.

The flow-cytometric examinations were carried out on formalin-fixed, paraffin-embedded thyroid tissue. The paraffin blocks were worked up according to the method of Hedley et al. (1985). The accuracy of this technique has been confirmed in 2 recent studies (Fossa et al. 1986; Franzen et al. 1986). From each block 5–10 slides of ≈8–10 µm thickness were prepared and exposed to xylol at 37° C for 30 min. After 30 min the xylol solution was changed, and the procedure was repeated. Then the samples were passed to an alcohol series from 100% to 95% to 70% to 50%, and finally submitted to destilled water. The tissue specimens were minced by scissors in 1 ml 0.25% pepsin in physiological saline containing 0.25% hydrochloric acid, followed by 3–5 min of automated agitation at room temperature. After 30 s of sedimentation, 0.5 ml of the supernatant suspension of nuclei were added to 10 ml of a fluorochrome solution consisting of 0.5 µg DAPI (4′-6-diamidino-2-phenylindole) + 20 µg RNase from bovine pancreas (100 Kunitz units/mg) per ml in 0.1 M tris-buffer solution at pH 7.6. The staining time was 15 min. The measurements of the DNA-dependent fluorescence were performed with an ICP 22 cytometric device (PHYWE AG, Göttingen). The electronic pulses were registered and analyzed by a multichannel analyzer, the measurement data were transferred to a graphic computer system, and from each sample 20,000 to 50,000 nuclear pulses were accumulated in the histograms. At first a logarithmic histogram was obtained on the screen, which was submitted to correction for background pulses (Beck 1980; Haag 1980) and transformed into an arithmetic histogram. The corrected histograms and the corresponding cumulative frequencies were printed out and used for the estimation of the cell cycle phases G0, G1, S, G2 and M. Flow cytometric histograms with a single peak were interpreted as representing a diploid tumour. In the presence of

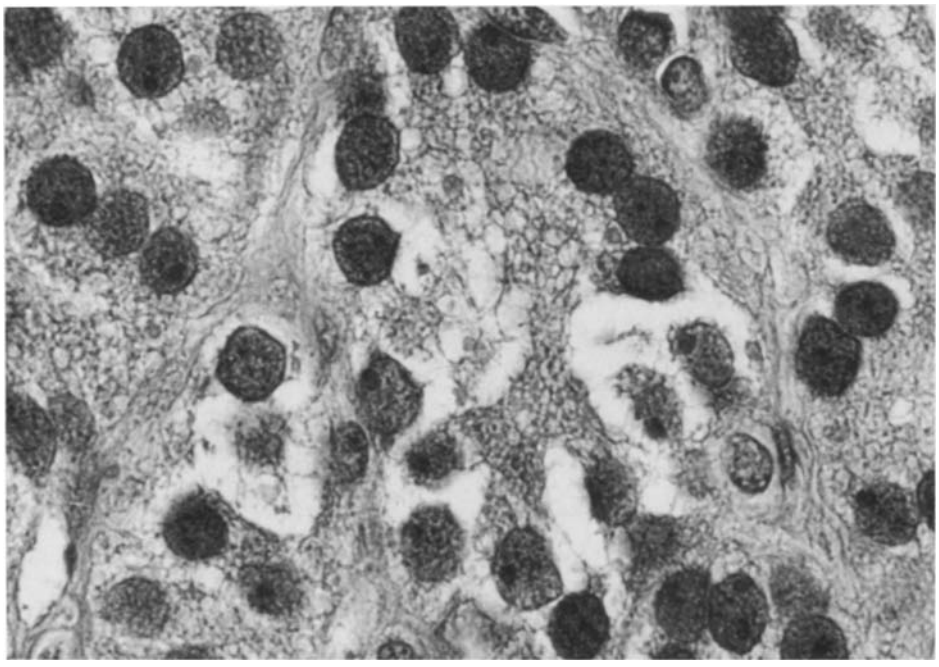

**Fig. 4.** Comparable region within a well-differentiated follicular carcinoma of the thyroid gland. Clear-cut cytological hallmarks of malignancy are lacking. Hematoxylin/Eosin. Oil immersion. Final magnification: 1,430×

**Table 1.** Stereological data: comparison of follicular adenomas and well-differentiated follicular carcinomas

| Estimate | Follicular adenomas ($n=15$) Mean ± SEM | Well-differentiated follicular carcinomas ($n=15$) Mean ± SEM | Level of statistical significance |
|---|---|---|---|
| 1. Primary morphometric data | | | |
| Mean TCN profile area [$\mu m^2$] | 38.43 ± 1.77 | 34.66 ± 1.48 | N.S. |
| Mean TCN profile perimeter [$\mu m$] | 22.45 ± 0.48 | 21.50 ± 0.43 | N.S. |
| Ratio: short/long TCN profile axis | 0.815 ± 0.005 | 0.781 ± 0.009 | $P<0.005$ |
| CV of TCN profile area | 0.244 ± 0.011 | 0.291 ± 0.014 | $P<0.02$ |
| Number of TCN profiles/tumour cell area [$mm^{-2}$] | 3,758 ± 216 | 4,189 ± 209 | N.S. |
| 2. Stereological estimates | | | |
| Volume density of TCN per tumour cell volume, $V_V$ [%] | 14.33 ± 0.68 | 14.15 ± 0.82 | N.S. |
| Surface density of TCN per tumour cell volume, $S_V$ [$\mu m^2/\mu m^3$] | 0.109 ± 0.005 | 0.113 ± 0.006 | N.S. |
| Surface-to-volume ratio of TCN [$\mu m^2/\mu m^3$] | 0.763 ± 0.017 | 0.805 ± 0.019 | N.S. |

an additional peak, the clearly defined peak with the lowest ploidy was considered as diploid (Fossa et al. 1986). The DNA index (*DI*) was defined as the ratio of the channel number of the abnormal peak to the channel number of the diploid peak (Figs. 1, 2). Tumours with $DI=1$ are diploid, and those with $1.1<DI<1.9$ and $2.1<DI$ were considered as aneuploid. Near-diploid tumours ($0.9\leq DI<1$; $1<DI\leq 1.1$), tetraploid tumours ($DI=2$), and near-tetraploid tumours were not found in our material. Cell clumping artifacts such as triplets were eliminated mathematically using a modification of a formula given by Beck 1980 (Feichter et al. 1985). The quality of the DNA histograms was controlled via the CV of the first peak: if it exceeded 5%, the preparation was repeated until a CV below 5% was obtained, or the data were excluded from the study.

Student's *t*-test for unpaired data was used for the comparison of group means. For the central morphometric parameter *A*, the precision was examined by nested analysis of variance, as described previously (Mattfeldt and Mall 1984; Mattfeldt et al. 1985a, b). Briefly, the total observed variance within groups between tumours is partly due to the "true" variance between tumours, $s_a^2$, and partly due to variance contributions from intra-tumour heterogeneity, i.e. the variance $s_f^2$ between the $n_f$ fields per case, and the variance $s_p$ between the $n_p$ individual profiles per field:

$$Os_a^2 = s_a^2 + s_f^2/n_f + s_p^2/(n_f n_p).$$

A result was considered to be statistically significant if the probability of error, *P*, was smaller than 0.05.

**Table 2.** Flow-cytometric findings and mean profile area of tumour cell nuclei in follicular adenomas and well-differentiated follicular carcinomas

| Adenomas | | | | | Carcinomas | | | | |
|---|---|---|---|---|---|---|---|---|---|
| No. | DI | %S | $\%G_2/M$ | Area | No. | DI | %S | $\%G_2/M$ | Area |
| 1 | 1.00 | 2.1 | 2.6 | 33.08 | 1 | 1.00 | 1.3 | 3.5 | 31.55 |
| 2 | 1.00 | 4.9 | 0.5 | 25.99 | 2 | 1.00 | 1.1 | 3.0 | 30.10 |
| 3 | 1.00 | 3.6 | 3.9 | 39.90 | 3 | 1.00 | 0.6 | 11.6 | 37.96 |
| 4 | 1.00 | 3.0 | 6.0 | 38.12 | 4 | 1.00 | 1.9 | 10.5 | 32.94 |
| 5 | 1.00 | 3.0 | 6.0 | 32.24 | 5 | 1.00 | 0.4 | 8.0 | 28.08 |
| 6 | 1.00 | 1.9 | 2.4 | 35.89 | 6 | 1.00 | 10.5 | 12.5 | 32.56 |
| 7 | 1.00 | 4.4 | 2.7 | 37.99 | 7 | 1.00 | 1.8 | 14.0 | 36.80 |
| 8 | 1.13 | 1.0 | 1.2 | 36.69 | 8 | 1.00 | 1.1 | 6.5 | 30.88 |
| 9 | 1.68 | 1.4 | 1.1 | 48.46 | 9 | 1.00 | 1.0 | 4.3 | 32.85 |
| 10 | 1.78 | 1.7 | 2.6 | 38.50 | 10 | 1.40 | 0.9 | 0.9 | 45.70 |
| 11 | 1.30 | 1.1 | 1.1 | 44.25 | 11 | 1.73 | 5.6 | 6.7 | 33.46 |
| 12 | 1.30 | 1.1 | 1.2 | 31.72 | 12 | 1.50 | 1.8 | 3.7 | 32.26 |
| 13 | 1.29 | 2.5 | 7.6 | 49.29 | 13 | 1.50 | 1.4 | 3.9 | 40.11 |
| Mean | | 2.44 | 2.99 | 37.86 | | | 2.26 | 6.85 | 34.25 |
| SEM | | 0.35 | 0.62 | 1.84 | | | 0.77 | 1.15 | 1.32 |
| Level of significance | | | | | | | N.S. | $P<0.01$ | N.S. |

*Abbreviations:* DI = DNA index, %S = percentage of cells in S-phase, $\%G_2/M$ = percentage of cells in $G_2$- and M-phase, Area = mean profile area of tumour cell nuclei ($\mu m^2$)

**Table 3.** Stereological data: comparison of diploid and aneuploid well-differentiated follicular tumours

| Estimate | Diploid follicular tumours ($n=16$) Mean ± SEM | Aneuploid follicular tumours ($n=10$) Mean ± SEM | Level of statistical significance |
|---|---|---|---|
| 1. Primary morphometric data | | | |
| Mean TCN profile area [$\mu m^2$] | 33.56 ± 0.98 | 40.04 ± 2.09 | $P<0.005$ |
| Mean TCN profile perimeter [$\mu m$] | 21.21 ± 0.32 | 23.10 ± 0.59 | $P<0.01$ |
| Ratio short/long TCN profile axis | 0.802 ± 0.009 | 0.800 ± 0.010 | N.S. |
| CV of TCN profile area | 0.251 ± 0.009 | 0.287 ± 0.021 | N.S. |
| Number of TCN profiles/tumour cell area [$mm^{-2}$] | 4,139 ± 229 | 3,795 ± 262 | N.S. |
| 2. Stereological estimates | | | |
| Volume density of TCN per tumour cell volume, $V_V$ [%] | 13.82 ± 0.86 | 14.71 ± 0.59 | N.S. |
| Surface density of TCN per tumour cell volume, $S_V$ [$\mu m^2/\mu m^3$] | 0.111 ± 0.006 | 0.109 ± 0.005 | N.S. |
| Surface-to-volume ratio of TCN [$\mu m^2/\mu m^3$] | 0.810 ± 0.012 | 0.744 ± 0.020 | $P<0.01$ |

## Results

Subjective examination of the neoplasms at high magnification failed to disclose any convincing differences between nuclear details in the adenoma group when compared with the carcinoma group (Figs. 3, 4). Eleven patients in the adenoma group were female, and 9 patients in the carcinoma group were female. Further results are displayed in the Tables 1–4 and may be summarized as follows. Adenomas and carcinomas do not differ significantly in estimates related to TCN size, i.e. mean TCN profile area, mean TCN profile perimeter, and the TCN surface-to-volume ratio. However, a decrease of the ratio: short/long profile axis, and an increase of the coefficient of variation (CV) of the TCN profile areas could be demonstrated in the malignant tumours. These findings are compatible with the interpretation that the axial ratio of the TCN decreases in the carcinoma group (the TCN are more unequiaxed here), and that the size variability of the TCN (anisokaryosis) is increased in the

**Table 4.** Nested analysis of variance for TCN profile area

| Group | Mean [$\mu m^2$] | Total observed variance between cases, $O_s a^2$ [$\mu m^4$] | Relative contributions to $O_s a^2$ by: | | |
|---|---|---|---|---|---|
| | | | Biological variation | Heterogeneity within neoplasms between fields | Heterogeneity within fields between profiles |
| Adenomas | 38.43 | 46.79 | 88% | 11% | 1% |
| Carcinomas | 34.66 | 32.83 | 78% | 21% | 1% |

malignant tumours. Diploid and aneuploid tumours were found in both groups with similar frequency (adenomas: 7 diploid, 6 aneuploid neoplasms; carcinomas: 9 diploid, 4 aneuploid neoplasms). In the separately investigated group of 6 aneuploid follicular adenomas the 24–80 additional sections per case failed to provide clear-cut evidence of angioinvasion or capsular penetration, and all patients were free from local recurrence and metastases. It was thus decided to leave the initial benign diagnosis unchanged. No significant difference between adenomas and carcinomas was detected with respect to the percentage of tumour cells in S-phase. However, the percentage of tumour cells in G2/M-phase was more than twice as high in the carcinoma group. Table 3 shows data that result from pooling the adenomas and carcinomas and subsequently dichotomizing the sample with respect to the state of ploidy. All estimates related to TCN size are significantly increased in the aneuploid group, whereas no changes of size variability and shape can be detected. Nested analysis of variance for TCN profile area (Table 4) shows that the largest contribution to the total observed variance within groups between tumours is provided by the true biological variation ("inter-individual differences"). Whereas a certain heterogeneity between different tumour regions cannot be denied, the heterogeneity between individual profiles only contributes about 1% of the total variance.

## Discussion

In the present study no significant difference between mean TCN profile area of follicular adenomas and well-differentiated follicular carcinomas could be detected. This result could, in principle, be either due to inaccurate morphometric techniques (the groups are in fact different, but we are unable to detect this because the variance between measurements within individuals is too high), or due to the fact that there is indeed no difference of TCN profile area in the adenoma and carcinoma populations. Nested analysis of variance (Table 4) shows that the former explanation is most unlikely: with the number of nuclear profiles studied here (150–250 per case), the largely preponderant portion of total observed variance (78–88%) is contributed by the true biological variation between individuals – and this quantity cannot be reduced even by complete serial section reconstruction of the whole tumour. Consequently morphometric estimation of mean TCN profile area is not a useful tool for the differential diagnosis of these conditions. This view is in agreement with the majority of previous studies (Georgii 1977; Lang et al. 1977; Mikuz et al. 1977; Schuh et al. 1980; Droese et al. 1981; Luck et al. 1982; Johannessen et al. 1983; Kriete et al. 1983; Schuh et al. 1984; Kriete et al. 1985). In contrast, one group found that planimetry of nuclear area in aspirated tumour cells could differentiate between follicular adenomas and follicular carcinomas: the projected nuclear areas in the carcinoma group were consistently larger than those of the adenoma group (Boon et al. 1980; 1982). The reason for this discrepancy could be that Boon et al. might have included also moderately differentiated carcinomas into their study. We have shown that aneuploid follicular tumours display a significantly higher mean TCN profile area than diploid follicular tumours (Table 3). This result corroborates earlier findings of our group in mammary carcinomas, where an increase of TCN size could be demonstrated in aneuploid as compared to diploid carcinomas (Möller et al. 1985). If moderately differentiated follicular carcinomas tend to a higher degree of aneuploidy than adenomas, as might well be the case, the inconsistency of the findings could partly be explained in terms of ploidy-related nuclear size differences.

We found 7 diploid versus 6 aneuploid follicular adenomas, and 9 diploid versus 4 aneuploid well-differentiated follicular carcinomas. Thus, our results reproduce the finding of other groups that it is not possible to discriminate between the 2 types of well-differentiated follicular neoplasms

by the criterium of ploidy (Haemmerli 1970; Rabenhorst 1974; Mikuz et al. 1977; Sprenger et al. 1977; Tschahargane et al. 1978; Johannessen et al. 1982). The percentage of cells in *S*-phase also did not differ significantly between the neoplasms. However, the percentage of cells in G2/M-phase was more than twice as high in carcinomas than in adenomas; a similar tendency has been reported in a small sample of cases recently (Johannessen et al. 1982). But again, the overlap of the data from individual cases prevents the use of this parameter as a diagnostic criterium.

Whereas TCN size apparently remains unchanged in carcinomas, we found that other morphometric estimates differed significantly between the 2 groups. The combined changes of the axial ratio of the profiles and the CV of TCN profile area suggest that nuclear size distribution and nuclear shape are altered in the carcinoma group. To specify these changes *numerically* in terms of the true, 3-dimensional alterations is not feasible from the present data in full detail. Such an analysis necessitates either (1) indirect, mathematical reconstruction of the bivariate particle size-shape distribution from the profile size-shape distribution under a certain geometric model assumption (e.g., biaxial spheroids: Cruz-Orive 1976; Weibel 1980), or (2) direct quantitative serial-section analysis of the particles (Cruz-Orive 1980; Mattfeldt and Mall 1983). Both approaches require thin sections (actual thickness much smaller than that of paraffin sections) and are time-consuming procedures, as mathematical reconstruction of ellipsoids in a bivariate size-shape distribution requires many hundreds of profiles to be analyzed and as serial section analysis requires accurate superposition and tracing of nuclei in a complete sequence of sections. Despite these limitations, it can be qualitatively inferred from the data that the TCN in carcinomas are more variable in size and possess a higher eccentricity. Clearly the increased anisokaryosis in carcinomas is in agreement with the cytometric findings: when a significantly higher percentage of cells is in G2-phase or in the mitotic phase, respectively, it follows that the amount of chromosomes and DNA per nucleus becomes more variable. This should in turn be reflected by an increased nuclear size variability, as the concentration of DNA per $\mu m^3$ nucleus volume has been reported to remain nearly constant despite large changes of nuclear size (Tasca and Stefaneanu 1977).

The present study has disclosed significant differences between follicular adenomas and well-differentiated follicular carcinomas. However, neither subjective evaluation of nuclear characteristics, nor stereology (morphometry), nor flow cytometry made possible a clear-cut separation of benign and malignant follicular neoplasm which could be applied in the differential diagnosis of individual patients. Moreover, descriptive and quantitative transmission electron microscopy, immunohistochemistry, and scanning electron microscopy have also all failed as diagnostic tools (Johannessen and Sobrinho-Simoes 1983). Several plausible reasons for the considerable overlap of data between groups should be considered. Let us consider a follicular neoplasm without visible capsular and vascular invasion on the slides examined. If this neoplasm has not metastasized at the moment when the thyroid nodule is resected, we would call it an adenoma, i.e. a benign encapsulated epithelial neoplasm. But as all cellular properties are not distinctive, it is by no means excluded that the neoplasm is not in fact a malignant tumour that has not yet begun infiltrative growth, i.e. a preinvasive carcinoma. Some authors suggested this more than 30 years ago and asked whether certain thyroid adenomas are in reality encapsulated adenocarcinomas without apparent vascular invasion (Hazard and Kenyon 1954). They considered preinvasive malignancy to be a biological entity especially in adenomas of markedly atypical character. This proposal would immediately resolve the contradiction that the "adenomas" are so often aneuploid. Moreover, it would provide an easy explanation for the fact that all the numerous and expensive efforts at a sharp distinction between the 2 conditions have failed. When the entity "adenoma" is heterogeneous and comprises an unknown percentage of preinvasive carcinomas, all attempts at a dichotomic separation from the group of the invasive carcinomas are artificial and bound to failure. It is equally plausible to think over this argument in the reverse direction: If follicular carcinoma has a preinvasive stage, then this precursor must be a neoplasm which – at a certain phase of development – already possesses all the cytological properties of a malignant tumour, but has not yet infiltrated the capsule and the vessel walls. In other words: if a preinvasive stage of follicular carcinoma exists, we cannot but denote it as an "adenoma" according to the established nomenclature. The reader should note that other examples exist where the term "adenoma" has been replaced by "carcinoma" from similar reasons. We quote here only "papillary adenoma" of the thyroid gland, which is now considered in most if not all cases as a papillary carcinoma (Hedinger and Sobin 1974; Vickery 1983; Schröder et al. 1984a).

Consequently it has been suggested that we should classify aneuploid follicular tumours in the absence of vascular or capsular invasion with pronounced cellular atypia as noninvasive follicular carcinoma (Greenebaum et al. 1985).

Another reason which might account for the broad overlap between groups may be due to a borderline histopathological appearance. The safe recognition of true capsular invasion is difficult and not unequivocal in some cases: It is not usually possible to differentiate histologically between invasive islands and islands of non-invasive adenoma tissue that have been entrapped within the capsule due to capsular infolding or capsular fibrosis (Schröder et al. 1984b). Similar statements hold for true angioinvasion and pseudoinvasion of a blood vessel. The diagnostic problems are well documented in a recent study (Greenebaum et al. 1985). These authors sent slides from aneuploid follicular thyroid tumours to 6 reference pathologists for expert review. In each of 3 aneuploid tumours originally diagnosed as follicular adenoma, the expert opinions differed (first case: 3 adenomas versus 3 carcinomas; second case: 5 adenomas versus 1 carcinoma; third case: 1 follicular carcinoma, 1 follicular variant of papillary carcinoma). Finally, stereological and flow cytometric studies on the thyroid gland must take into consideration eventual differences in the functional state of the neoplasms. Subtle differences cannot be ruled out here, even if autonomous adenomas are excluded from the study; and minor differences in endocrine activity may well be correlated with quantitatively demonstrable nuclear alterations. It is well-known that the follicular epithelium may display very marked nuclear changes in benign diseases, e.g. diffuse hyperthyroidism. In a case of diffuse adenomatous goiter, even aneuploidy has been detected by flow cytometry (Johannessen et al. 1982). In our view, it seems most plausible that all these 3 components – unrecognized preinvasive malignancy in "adenomas", misclassification of some cases with borderline appearance, subtle functional changes – contribute to the considerable overlap of data and thus render diagnostic morphometry and flow cytometry of individual follicular thyroid tumours impracticable at present.

## References


Abramowitz M, Stegun IA (1964) Handbook of Mathematical Functions with Formulas, Graphs, and Mathematical Tables. Dover Publications, New York

Beck HP (1980) Evaluation of flow cytometric data of human tumors. Correction procedures for background and cell aggregations. Cell Tissue Kinet 13:173–181

Böcker (1984) Schilddrüse. In: Pathologie 3, ed. Remmele W, Springer, Berlin Heidelberg New York, pp 415–445

Boon ME, Löwhagen T, Willems JS (1980) Planimetric studies on fine needle aspirates from follicular adenoma and follicular carcinoma of the thyroid. Acta Cytol 24:145–148

Boon ME, Löwhagen T, Lopes Cardozo P, Blonk DI, Kurver PJH, Baak JPA (1982) Computation of preoperative diagnosis probability for follicular adenoma and carcinoma of the thyroid on aspiration smears. Anal Quant Cytol 4:1–5

Chen KTK, Rosai J (1977) Follicular variant of thyroid papillary carcinoma: A clinicopathologic study of six cases. Am J Surg Pathol 1:123–130

Cruz-Orive LM (1976) Particle size-shape distributions: the general spheroid problem. I. Mathematical model. J Microsc 107:235–253

Cruz-Orive LM (1980) On the estimation of particle number. J Microsc 120:15–27

Droese M (1979) Aspirationszytologie der Schilddrüse. Schattauer, Stuttgart

Droese M, Mentgen-Nothum V, Eins S, Klar R (1981) Morphometrische Dignitätsbeurteilung follikulärer Schilddrüsentumoren im Feinnadelpunktat. Verh Dtsch Ges Pathol 65:384

Feichter GE, Kühn W, Czernobilsky B, Müller A, Heep J, Abel U, Haag D, Kaufmann M, Rummel HH, Kubli F, Goerttler K (1985) DNA flow cytometry of ovarian tumors with correlation to histopathology. Int J Gynecol Pathol 4:336–345

Fossa SD, Thorud E, Shoaib MC, Pettersen EO (1982) DNA flow cytometry of cells obtained from old paraffin-embedded specimens. A comparison with results of scanning absorption cytometry. Pathol Res Pract 181:200–205

Franzen G, Olofsson J, Risberg B, Klintenberg C, Nordenskjöld B (1986) DNA measurements on formalin-fixed, paraffin-embedded squamous cell carcinomas from different ENT-regions. Pathol Res Pract 181:230–235

Georgii A (1977) Die epithelialen Tumoren der Schilddrüse. Verh Dtsch Ges Pathol 61:191–208

Greenebaum E, Koss LG, Elequin F, Silver CE (1985) The diagnostic value of flow cytometric DNA measurements in follicular tumors of the thyroid gland. Cancer 56:2011–2018

Haag D (1980) Flow microfluorimetric deoxyribonucleic acid (DNA) analysis supplementing routine histopathologic diagnosis of biopsy specimens. Lab Invest 42:85–90

Haemmerli G (1970) Zytophotometrische und zytogenetische Untersuchungen an knotigen Veränderungen der menschlichen Schilddrüse. Schweiz Med Wochenschr 100:633–641

Hazard JB, Kenyon R (1954) Atypical adenoma of the thyroid. Arch Pathol 58:554–563

Hedinger C, Sobin LH (1974) Histological Typing of Thyroid Tumors. World Health Organization, Geneva

Hedley DW, Friedlander ML, Taylor IW, Rugg CA, Musgrove EA (1983) Method for analysis of cellular DNA content of paraffin embedded pathological material using flow cytometry. J Histochem Cytochem 31:1333–1335

Johannessen JV, Sobrinho-Simoes M, Lindmo T, Tangen KO (1982) The diagnostic value of flow cytometric DNA measurements in selected disorders of the human thyroid. Am J Clin Pathol 77:20–25

Johannessen JV, Sobrinho-Simoes M (1983) Well differentiated thyroid tumors. Problems in diagnosis and understanding. Pathol Annu 18:255–285

Johannessen JV, Sobrinho-Simoes M, Finseth I, Pilström L (1983) Ultrastructural morphometry of thyroid neoplasms. Am J Clin Pathol 79:166–171

Kriete A, Romen W, Schäffer R, Harms H, Haucke M, Gerlach B, Aus HM, ter Meulen V (1983) Computer analysis of

chromatin arrangement and nuclear texture in follicular thyroid tumors. Histochemistry 78:227–230
Kriete A, Schäffer R, Harms H, Aus HM (1985) Computer-based cytophotometric classification of thyroid tumors in imprints. J Cancer Res Clin Oncol 109:252–256
Lang W, Georgii A, Atay Z (1977) Differentialdiagnose zwischen atypischem Adenom und follikulärem Carcinom der Schilddrüse. Verh Dtsch Ges Pathol 61:275–279
Lang W, Georgii A, Stauch G, Kienzle E (1980) The differentiation of atypical adenomas and encapsulated follicular carcinomas in the thyroid gland. Virchows Arch A [Path Anat Histol] 385:125–141
Lang W, Choritz H, Hundeshagen H (1986) Risk factors in follicular thyroid carcinomas. A retrospective follow-up study covering a 14-year period with emphasis on morphological findings. Am J Surg Pathol 10:246–255
Löwhagen T, Sprenger E (1974) Cytologic presentation of thyroid tumors in aspiration biopsy smear. A review of 60 cases. Acta Cytol 18:192–197
Luck JB, Mumaw VR, Frable WJ (1982) Fine needle aspiration biopsy of the thyroid. Differential diagnosis by videoplan image analysis. Acta Cytol 26:793–796
Mattfeldt T, Mall G (1983) Dipyridamole-induced capillary endothelial cell proliferation in the rat heart – a morphometric investigation. Cardiovasc Res 17:229–237
Mattfeldt T, Mall G (1984) Estimation of length and surface of anisotropic capillaries. J Microsc 135:181–190
Mattfeldt T, Möbius HJ, Mall G (1985a) Orthogonal triplet probes: an efficient method for unbiased estimation of length and surface of objects with unknown orientation in space. J Microsc 139:279–289
Mattfeldt T, Neurohr W, Müller A, Klinga K (1985b) Morphometrische Korrelate des Steroidrezeptorengehaltes duktalinvasiver Mammakarzinome. Verh Dtsch Ges Pathol 69:350–355
Mattfeldt T, Neurohr W, Müller K, Klinga K (1985c) Stereologic correlates of steroid receptor concentration in invasive ductal breast cancer. Anal Quant Cytol Histol 7:310–314
Mikuz G, Hofstädter F, Schwarzlmüller B (1977) Feulgenzytophotometrische Untersuchungen an „falsch" und „richtig positiven" zytologischen Präparaten von Feinnadel-Schilddrüsenpunktaten. Verh Dtsch Ges Pathol 61:290–294
Miles RE, Davy P (1976) Precise and general conditions for the validity of a comprehensive set of stereological fundamental formulae. J Microsc 107:211–226
Möller P, Gross C, Feichter G, Mattfeldt T, Kaufmann M (1985) Vergleich von Bindungsmustern etablierter und neuer monoklonaler Antikörper, von Antiseren und Lektinen mit impulscytophotometrischen und morphometrischen Parametern und dem Hormonrezeptorstatus am Mammacarcinom. Verh Dtsch Ges Pathol 69:405–408
Rabenhorst G (1974) The diagnostic value of the DNA content of fine needle biopsies of the thyroid gland. Virchows Arch B [Cell Pathol] 16:379–383
Schröder S, Böcker W, Dralle H, Kortmann KB, Stern C (1984a) The encapsulated papillary carcinoma of the thyroid. A morphologic subtype of the papillary thyroid carcinoma. Cancer 54:90–93
Schröder S, Pfannschmidt N, Dralle H, Arps H, Böcker W (1984b) The encapsulated follicular carcinoma of the thyroid. A clinicopathologic study of 35 cases. Virchows Arch A [Pathol Anat] 402:259–273
Schuh D, Steidl R, Voß K (1980) Unterscheidung von follikulären Adenomen und Karzinomen in der Schilddrüsenfeinnadelbiopsie durch computergestützte zytomorphometrische Untersuchungen. Zentralbl Allg Pathol Pathol Anat 124:557–560
Schuh D, Steidl R, Mende T, Schneider H, Reske W (1984) Ergebnisse der automatischen Mikroskopbildanalyse von Schilddrüsenfeinnadelbiopsien. Zentralbl Allg Pathol Pathol Anat 129:35–41
Sprenger E, Löwhagen T, Vogt-Schaden M (1977) Differential diagnosis between follicular adenoma and follicular carcinoma of the thyroid by nuclear DNA determination. Acta Cytol 21:528–530
Tasca C, Stefaneanu L (1977) Cytology and cytophotometry in thyroid diseases. Acta Histochem 60:261–272
Tschahargane C, Goerttler K, Ehemann V, Haag D (1978) Application of flow-through DNA measurements in thyroid diseases. Pulse Cytophotometry 3:527–532
Vickery AL (1983) Thyroid papillary carcinoma. Pathological and philosophical controversies. Am J Surg Pathol 7:797–807
Weibel ER (1979) Stereological Methods. I. Practical Methods for Biological Morphometry. Academic Press, London
Weibel ER (1980) Stereological Methods. II. Theoretical Foundations. Academic Press, London

Accepted November 16, 1986